

**The Experimental Set-Up of a Triple-Sensor  
Anemometry and its Controlling System  
at the High-Speed Cascade Wind Tunnel**

**D. Wunderwald, G. Wilfert, L. Fottner  
Universität der Bundeswehr München, Germany**

### **Abstract:**

The investigation of transitional, partly separated boundary layers in highly loaded cascades requires a measuring technique to register the three-dimensional character of the turbulent flow. The concept of this measuring technique, a multiple hot-sensor anemometry, is the object of this paper.

Beside the selection of the hardware components the development of an extensive software was necessary. Therefore the acquisition of the upcoming measuring signals, the way of saving these data, the processing and the possibilities of evaluation are important criteria that have to be considered.

The controlling program named SMASH (software

for masurement and analytical evaluation of signals from hot-sensor anemometry) consists of several modules and provides a powerful tool for all steps from configuring the whole experimental set-up to the output of the evaluation results.

Problems in calibrating triple-sensor probes will be discussed. A simplified traversing unit is presented. Especially the influences of pressure, temperature and Mach number on the calibration results are pointed out. Calibration errors due to the procedure are estimated and calculated flow properties are compared.

## Contents:

### Nomenclature

1. Introduction
2. Concept of the 3D Hot-Sensor Anemometry - Setup at the High-Speed Cascade Wind Tunnel
  - 2.1 The Experimental Setup of the Hot-Film Data Acquisition System
  - 2.2 The Peripheral Data Acquisition System
  - 2.3 The Software for Measurement and Analytical Evaluation of Signals from Hot-Sensor Anemometry (SMASH)
3. The Calibration of Triple Hot-Sensor Probes
  - 3.1 The Influence of Different Measurement Parameters on Calibration Results
4. Conclusions
5. Acknowledgements
6. References
7. List of Figures

## Nomenclature

### a) Symbols:

$a_i$		directional calibration coefficients
$c_i$		velocity calibration coefficients
$k_1, k_2$		influence factors
$u$	[mm]	coordinate in circumf. direction
$x$	[mm]	coordinate in flow direction
$z$	[mm]	coordinate in spanwise direction
$\alpha$	[°]	yaw angle of the probe
$\beta$	[°]	pitch angle of the probe
$\varphi$	[°]	roll angle of the probe
$A, B, n$		calibration coefficients
$E$	[V]	anemometer output voltage
$Nu$	[-]	Nusselt number
$Tu$	[%]	degree of turbulence
$Re$	[-]	Reynolds number
$U, V, W$	[m/s]	components of velocity vector $\underline{U}$ in probe-fixed coordinate system
$UQ$		velocity quotient

### b) Indices:

cal	calculated
e	normalized effective
eff	effective
err	relative error quantity
s	sensor-fixed coordinate system
trav	traversed
D	computed with directional approach
V	computed using the velocity calibration

### c) Abreviations:

1D, 3D	one dimensional, three dimensional
CTA	<u>C</u> onstant <u>T</u> emperature <u>A</u> nemometry
DLR	<u>D</u> eutsche <u>F</u> orschungsanstalt für <u>L</u> uft- und <u>R</u> aumfahrttechnik
HFA	<u>H</u> eißfühler- <u>A</u> nemometrie (hot-sensor a.)
IEEE	Institute of <u>E</u> lectrical and <u>E</u> lectrical <u>E</u> ngineers
ISA	<u>I</u> nstitut für <u>S</u> trahlantriebe (UniBwM)
SMASH	<u>S</u> oftware zur <u>M</u> essung und <u>A</u> uswertung von <u>S</u> ignalen der <u>H</u> eißfühler- <u>A</u> nemometrie (Software for <u>M</u> easurement and <u>A</u> nalitical <u>E</u> valuation of <u>S</u> ignals from <u>H</u> ot-Sensor Anemometry)
UniBwM	<u>U</u> niversität der <u>B</u> undesweh <u>r</u> <u>M</u> ünchen

## 1. Introduction

The aerodynamic optimization of compressor and turbine blades leads to a further increased blade loading while optimized designs of turbo components lead to computer programs which take into consideration as many effects as possible. One of these effects which still represents a big problem is the realistic modelling of turbulence for the calculation of the turbulent flow. A customary method to investigate these problems experimentally in a wind tunnel is to use a plane cascade model.

The High-Speed Cascade Wind Tunnel of the University of the Federal Armed Forces Munich (Fig. 1.1) is installed in a tank, which can be evacuated up to 40 hPa and pressurized up to 1200 hPa, so that an independent variation of Mach and Reynolds number is possible. The rebuilding of the wind tunnel, which was formerly in operation at the DLR in Braunschweig, was finished in November 1985 (see /1/). After some calibration tests the establishment of different measuring techniques started simultaneously with the research work (see /2/). One of the main topics of this work are investigations on the losses of turbomachine blades and on the boundary layer behavior.

The multidimensional hot sensor technique is a necessary supplement of the existing measuring technique on the High-Speed Cascade Wind Tunnel. Up to now, already a 1D-hot-sensor technique was installed and tested. Experience was gained with this system, but the limitations of this system were soon obvious, since the computing power of the installed computer as well as the software made the off-line evaluation of the test data impossible. Thus it was decided to extend the existing 1D-technique to a multidimensional technique and to increase the data storage and computing power extensively. Efficient computer programs had to be prepared for the control of the measurement system, the control of the large amount of test data, and for the documentation of the tests in a respectable manner.

Extensive tests especially on the accuracy of the velocity and directional calibration procedure were carried out. The influence of different measurement parameters, e.g. recording time, cutoff-frequency, temperature- and pressure variation on the calibration results will be presented in this paper.

## 2. Concept of the 3D-Hot-Sensor Anemometry - Setup at the High-Speed Cascade Wind Tunnel

The hot-wire/hot-film technique is based on the principal of heat transfer between a cylinder and the flow around it. While the mean element of a hot-wire probe is a thin sensor of 2.5 to 5  $\mu\text{m}$  diameter made of platinum or tungsten the sensor of a hot-film probe consists of a thin coating of 0.5  $\mu\text{m}$  on a crystal cylinder of 70 - 200  $\mu\text{m}$  diameter.

The wire is heated by an electrical current and cooled by the flow. Thus a change of velocity causes a variation of the sensor's temperature. In a constant temperature hot-wire anemometer system which is used at the institute, the temperature of the sensor is kept constant by amplification of the error signal of the bridge which changes the measured supply voltage of the bridge (see Fig. 2.1). The system is limited to a maximum frequency of 70 kHz, but in this case the cutoff-frequency is not higher than 25 kHz. More details about the system can be found in /3/,/4/.

The sensor of the 3D-Hot-Film Anemometry (3D-HFA) consists of three spatially stretched wires or films. These sensors are used in various sizes depending on measuring tasks. However even when using very thin wires the smallest sensor still needs a measuring volume of 1 mm<sup>3</sup>. The two triple probes used at the High-Speed Cascade Wind Tunnel and a test object is shown in Fig. 2.2.

The setup of the 3D-HFA at the High-Speed Cascade Wind Tunnel is based on a "digital solution" which means that the analog output signal of the anemometer is digitized, filtered, and stored on a hard disk. After the measurement the stored data can be subsequently evaluated.

Figure 2.3 shows the hardware setup of the 3D-HFA which can be divided in three parts:

- the hot-film-digitization with the direct storing on a fast hard disk (Through-Put-Disk)
- the peripheral data measurement controlled by an IEEE-Bus for temperatures, pressures, traversing coordinates, etc.
- the monitoring of the anemometer output signal by using two voltmeters for AC and DC, an oscilloscope and a fast-fourier-analyzer

## 2.1 The Experimental Setup of the Hot-Film Data Acquisition System

As mentioned before the experimental setup consists of three sections. In the first part the analog output signals of the three anemometers have to be digitized, filtered and stored. The hardware for this task is an optimized system of an A/D-converter with an anti-aliasing-filter and a digital filter with zoom function which allows a converting-frequency only 2.56 times higher than the cutoff-frequency. All three modules are always working with an internal sample rate of 262 kHz but if lower cutoff-frequencies are wanted the data are recorded only partially. For measurements with the anemometer system a cutoff-frequency of 25.6 kHz or 12.8 kHz is normally used. The 14 bit A/D-converter of the system achieves a high resolution with a relative error of 0.024% for DC- and AC-measurements (see [Fig. 2.4](#)).

When setting up the HFA-system the record time of the anemometer signals necessary for a calibration or a cascade measurement could only be estimated. Therefore it was set up with the possibility of very long record times. This was achieved by storing the digitized signals directly on a fast hard disk with a maximum transfer rate of 900 kbytes/s. With a storage capacity of 150 MBytes and a "compression factor" of about 2 very long record times e.g. 30 seconds can be realized for some shots before a transfer to the magneto-optical-disk is necessary. These long record times were spent on turbulence measurements with the 1D-HFA which is also installed at the High-Speed Cascade Wind Tunnel.

## 2.2 The Peripheral Data Acquisition System

In addition to the hot film signals a lot of other data (peripheral data) have to be recorded, e.g. pressures, temperatures, traversing coordinates, etc.. A hard- and software is used that was developed and tested for wake and profile pressure distribution measurements at the institute /5/.

For temperature measurements Pt100 platinum resistance thermometers are used. Up to 6 thermometers can be installed at different positions in the wind tunnel, e.g. in the settling chamber, in the measuring cross section, etc.. The signals of the thermometers are scanned to a digital voltmeter, which is connected with the host computer by an IEEE-Bus.

The system DPT-6400 enables the measurement of up to 24 differential pressures in six different ranges from 25 hPa up to 1000 hPa. A fully automatical zero and span calibration or only a zero offset calibration of all transducers is supported by the operating

system of the DPT-6400. The calibration pressures for the transducers are generated by two digital pressure controllers. The digital barometer measures the barometric pressure as a reference for all pressure measurements (see [Fig. 2.5](#)).

The traversing system at the High-Speed Cascade Wind Tunnel for a triple hot-film probe has five motor driven axis and one additional, manual adjustable axis for moving the probe behind or in between the cascade. The five motor driven axis are (see [Fig. 2.6](#)):

- x-axis = linear axis in flow direction
- z-axis = linear axis in spanwise direction
- u-axis = linear axis in circumferential direction
- $\beta$ -axis = axis of rotation around the z-axis
- $\varphi$ -axis = axis of rotation around the probe axis

Triple hot film probes have to be calibrated not only for the velocity- but also for the directional sensitivity. For the directional calibration the probe has to be rotated around the z-axis (pitch angle) and the u-axis (yaw angle) at the same flow conditions. A rotation of the probe around the z-axis is already installed. To prevent a complicate modification for the variation of the yaw angle a simple method is to rotate the probe around it's own axis (roll angle  $\varphi$ ) and obtain the pitch and yaw angle by a coordinate transformation of the adjusted angle  $\varphi$  and  $\beta$  (see [Fig. 2.6](#)). A system of position and control units in the control room of the test facility was designed for computer or manual remotely controlled movement of the probe. Using the program modules the position accuracy is 0.04 mm for linear axis, 0.02° for the  $\beta$ -axis, and 0.1° for the  $\varphi$ -axis. A detailed description of the extended traversing system is given in /6/,/7/. [Figure 2.7](#) shows the traversing arm of the hot-sensor probes.

## 2.3 The Software for Measurement and Analytical Evaluation of Signals from Hot-Sensor Anemometry (SMASH)

In order to control the acquisition system and to evaluate the signals of the hot-film anemometry a program package was developed (SMASH). This software is highly modular and flexible for many different test applications. When programming the software parts of the software for wake and profile-pressure distribution measurements, e.g. the configuration or the control of the peripheral data acquisition, were used. The program consists of five moduls (see [Fig. 2.8](#)):

- the configuration module
- the calibration module
- the measurement module

- the evaluation module
- and the documentation module

In the configuration module all cascade data, the data of the experimental setup and the actual test-specific data can be controlled or changed before the next experiment is performed.

In the second program module a triple hot film probe can be calibrated for velocity- and directional sensitivity. The procedure to calculate the velocity and directional coefficients was developed at DLR-Göttingen. An advantage of this procedure is the possibility to calibrate the velocity- and directional sensitivity separately. The evaluation can be performed on- or off-line to obtain the calibration coefficients.

After reading configuration and calibration data a measurement can be carried out. For every measuring point of the traversing program data are obtained which are written on the through-put-disk in a compressed binary manner. During the traversing to the next point these data are reread and stored on the magneto-optical-disk together with the peripheral data to be evaluated off-line later.

The evaluation module, also part of the DLR-developed program, transforms the anemometer voltages to the velocity vector using the calibration coefficients of the second module. Fluctuations of the flow velocity with respect to time are measured with a sufficiently high frequency in order to calculate the degree of turbulence as well as the Reynolds stress tensor.

The last module performs the documentation of the configuration and cascade data as well as the calibration coefficients and the results of the measurements.

### 3. The Calibration of Triple Hot-Sensor Probes

On account of the results reported in /8/, a procedure was chosen that allows the separate calibration of triple-sensor probes regarding their velocity-related and directional characteristics without the knowledge of the exact probe geometry. Using a probe-fixed coordinate system (see Fig. 2.2) with the x- axis along the major axis of the probe shaft, the components of the free-stream velocity  $\underline{U}$  are:

$$U = |\underline{U}| \cdot \cos\alpha \cdot \cos\beta \quad (3.1a)$$

$$V = |\underline{U}| \cdot \sin\alpha \cdot \cos\beta \quad (3.1b)$$

$$W = |\underline{U}| \cdot \sin\beta \quad (3.1c)$$

For a hot-sensor King's heat transfer law is /9/

$$Nu = A + B \cdot Re^n \quad (3.2)$$

where A,B and n are calibration constants.

If the probe's ambient pressure at the calibration agrees with the pressure at the actual measurement the measurable bridge voltage E can be described with a heat balance as

$$E^2 = A' + B' \cdot U^n \quad (3.3)$$

At a velocity calibration the effective cooling velocity  $U_{eff}$  is for each sensor of a not-inclined probe ( $\alpha, \beta = 0^\circ$ )

$$U_{eff} = |\underline{U}| = U \quad (3.4)$$

Suitably, equation (3.3) will be replaced by a fourth order polynomial:

$$U_{eff} = c_0 + c_1 E + c_2 E^2 + c_3 E^3 + c_4 E^4 \quad (3.5a)$$

To register the dependence of the sensor cooling from the flow direction, the relation suggested by Jørgensen /10/

$$U_{eff}^2 = U_s^2 + k_1 V_s^2 + k_2 W_s^2 \quad (3.6)$$

is widely used. The tangential and the binormal velocity components  $V_s$  and  $W_s$  in a sensor-fixed coordinate system are considered with the influence factors  $k_1$  and  $k_2$ .

Assuming that the directional characteristics of a probe remain relatively constant, only the velocity calibration has to be repeated more often because of a curve drift due to aging and fouling processes. The transformation of equation (3.6) to the probe-fixed coordinate system leads to the approach

$$U_{eff} = \bar{a}_1 U^2 + 2\bar{a}_2 UV + 2\bar{a}_3 UW + \bar{a}_4 V^2 + 2\bar{a}_5 VW + \bar{a}_6 W^2 \quad (3.7a)$$

The effective cooling velocity in equation (3.5a) still depends on the knowledge of the coefficients  $\bar{a}_i$ . Therefore a normalized effective cooling velocity  $U_e$  is used when performing a calibration without known directional coefficients ( $\alpha, \beta = 0^\circ$ ):

$$U_e^2 = U_{eff}^2 / \bar{a}_1 = |\underline{U}|^2 \quad (3.8)$$

The velocity coefficients  $c_i$  of the polynomial

$$U_e = c_0 + c_1 E + c_2 E^2 + c_3 E^3 + c_4 E^4 \quad (3.5b)$$

are computed using the least squares method for different pairs of values E(U).

For determination of the directional coefficients  $a_i$  the pitch and the yaw angle of the probe is varied at a constant free-stream velocity. The effective cooling velocities are calculated from the measured voltages and adjusting surfaces are computed again with the least squares method:

$$U_e = a_1 U^2 + 2a_2 UV + 2a_3 UW + a_4 V^2 + 2a_5 VW + a_6 W^2 \quad (3.7b)$$

By transforming the directional coefficients, a velocity calibration could be performed at nearly arbitrary flow angle.

The evaluation of hot-sensor measurements is performed with known coefficients  $c_i$  and  $a_i$  by computing the instantaneous velocity vector from the anemometer output signals /8/. On the assumption that the effective cooling velocity calculated with the equations (3.5b) and (3.7b) is ideally identical there are three equations for three unknown velocity components.

### 3.1 The Influence of Different Measurement Parameters on Calibration Results

Different influence parameters on ISA's 3D-hot-sensor anemometry were investigated within an extensive test program. In order to optimize this measuring technique for its use in cascade testing at the High-Speed Cascade Wind Tunnel the results of velocity and directional calibrations were analyzed for different settings /11/:

- a) Variation of wind tunnel-dependent parameters like tank pressure, settling chamber total temperature and upstream turbulence;
- b) Variation of measuring system-related parameters like data acquisition time, sampling rate and frequency span, etc;

The two mainly dominating influences on the results of a velocity calibration are shown in Fig. 3.1: When setting different Reynolds numbers independently at a certain Mach number by varying the tank pressure the density of the fluid is changed. With increasing density the heat transfer from the sensor to the fluid and thus the bridge voltage at the anemometer increases. The temperature of the fluid influences the calibration curve in the opposite direction: The control system of the anemometer keeps the sensor temperature constant when working with the CTA-method. Therefore at a higher temperature of the fluid a lower heat flux is transferred which leads to a lower voltage from the anemometer /12/,/13/.

The increase of the voltage input range e.g. from 12 dBVp to 18 dBVp or the variation of the voltage recording time between 200 ms and 1000 ms did not result in any changes of the calibration output. However these parameters play an important role for the accuracy and reproducibility of the evaluation of measurements, the calculation of the velocity vector and turbulence quantities.

Based on the evaluation of averaged measuring values for each velocity setting, the shape of the fitting velocity calibration curve within the interesting range is reproduced very well. Informations about

the different settings probably get lost within the averaging procedure. Below a free-stream velocity of about 20 m/s the calibration points are approximated insufficiently due to the limited compressor operating range and the pressure acquisition system chosen for higher dynamic pressures. The mean square deviation for the experimentally relevant approximation is about 1% before performing a correction concerning pressure and temperature fluctuations.

The adaption of the temperature corrections of Bearman /14/ and Kanevce, Oka /15/ that are already successfully applied at the single sensor anemometry (1D-HFA) enables a compensation of temperature deviations of  $\pm 10$  K. Fig. 3.2 shows a temperature correction. The remaining deviations of the calibration curves are caused by a slightly different setting of the tank pressure. A correction of these pressure influences, at the development stage within the scope of the 1D-HFA-testing, will be introduced also for this 3D-HFA.

Compared with a triple-wire probe DANTEC 55P91 the triple-film probe 55R91 of the same geometry and overheat ratio is much more sensitive for velocity changes (Fig. 3.3). The different behavior of the sensor curves results from a changed roll angle position to the probe shaft axis.

With a higher degree of the upstream turbulence also higher output voltages at a certain velocity were expected because of an increased heat transfer. However the calibration measurements with a built-in turbulence generator did not confirm that. It is assumed that the degree of turbulence is still too low (measured degree of turbulence  $Tu=3.5\%$ ) to have a significant influence on the calibration results.

The directional characteristics of the used probes are shown in Fig 3.4 The pitch and yaw angle were traversed from  $-25^\circ$  to  $+25^\circ$  in  $5^\circ$ -steps. The effective cooling velocity is computed from the measured voltages at Machnumber  $Ma=0.6$  using the velocity calibration and related to the absolute value of the free-stream velocity. The velocity quotient is

$$UQ = u_e / |\underline{u}| \quad (3.8)$$

The different characteristics for the sensors are again a result of the roll angle position to the probe shaft axis and thus to the probe-fixed coordinate system. Depending on the angle position of the probe to the free-stream, a different influence on the cooling of the sensor (respectively the effective cooling velocity) can be observed. The figures show the distribution of the related cooling velocity UQ depending on the traversed pitch and yaw angle.

Basically, these contour line plots form a bowl-like part of a curved surface. The almost exclusive sensitivity to a change of the pitch angle  $\beta$  of the wire probe's sensor 3 or the film probe's sensor 1 results from a position in a plane parallel to the x-y-plane. The slowly increasing sensitivity to the yaw angle indicates the inclination towards the y-axis. If the sensor is not located in a plane parallel to another plane of the coordinate system, the curved surfaces are turned and these sensors are sensitive towards both of the traversing angles.

The variation of the above mentioned parameters also showed the independence of the data acquisition system from (reasonable) changes in some HFA-settings, a fact that helps reducing calibration time and storage capacity. The reproducibility of the directional characteristics illustrates Fig 3.5, where beside some set-up parameters the traversed angles and stepwidths were changed. Because the isolines show measured data and not yet the adjusted surface there might appear certain instabilities in these isolines.

The computations of the directional characteristics from calibration tests at different temperatures and tank pressures indicate a fundamental independence of the behavior for each sensor. Differences in level or gradient of the formed surfaces can be explained by the used velocity calibrations: If the measured voltages are combined with a velocity calibration e.g. of a lower temperature, not only higher velocities  $U_e$  and thus UQ are computed but also the velocity differentials for two constant voltages increase because the calibration curves become less steep at higher velocities. In the areal representations of the related cooling velocity this fact is indicated by increasing gradients  $dUQ/d\alpha$  and  $dUQ/d\beta$  respectively. The effect on the gradient decreases with increasing tank pressure. It seems to be necessary to calibrate for the velocity and the directional sensitivity at the same conditions in the tank. The use of temperature corrigated measuring data should ensure an adjustment and the reproducibility. The influence on the surface's gradient described in the latter also results from a change in tank pressure.

Calibrations at different Mach numbers showed the influence of this important parameter. Fig. 3.6 presents the directional characteristics for  $Ma=0.15$  and  $Ma=0.6$ . The roll angle position of the probe was not exactly the same in both tests, so the plots have to be turned for about  $7^\circ$ . The strong decrease of the gradient as well as the curvature of the calibration surfaces with increasing Mach number is evident. It means the sensors lose some of its sensitivity and therefore the measurements probably don't have the same accuracy.

The above drawn comparisons were based on an effective cooling velocity calculated with equation (3.5b). Because the velocity calibration showed very good results the assumption should be justified that realistic directional characteristics of the probes are shown. For an estimation of errors of the directional coefficients (more or less computed with the same numerical algorithm) the effective cooling velocity was also calculated using equation (3.7b). The relative error of the related cooling velocities is

$$\frac{U_{Q_V} - U_{Q_D}}{U_{Q_V}} = \frac{\frac{U_{eV}}{|\underline{U}|} - \frac{U_{eD}}{|\underline{U}|}}{\frac{U_{eV}}{|\underline{U}|}} = \frac{U_{eV} - U_{eD}}{U_{eV}}$$

$$\frac{U_{eV} - U_{eD}}{U_{eV}} = U_{e, err} \quad (3.9)$$

and out of it the relative deviation  $U_{e, err}$  of the effective cooling velocity can be determined.  $U_{eV}$  is the computed value using the velocity calibration and  $U_{eD}$  is the theoretically equal velocity computed with the directional approach. Fig. 3.7 shows an example of the adjusted surfaces ( $U_{Q_D}$ ) for the calibration and the distribution of the relative deviation  $U_{e, err}$ . In those areas where the related cooling velocity reaches values lower than 0.7 the relative error increases to absolute higher values than 2%. Obviously the measured data are not approximated well enough in these regions.

The evaluation of the calibration data as hot-sensor measurements with known calibration coefficients gives a further impression the occurring effects. The evaluated flow properties of two different settings are presented in Fig. 3.8 (see also Fig. 3.5). In all cases the structures of the comparable distributions are very similar. The relative deviation of the calculated velocity

$$\frac{|U_{cal}| - |\underline{U}|}{|\underline{U}|} = U_{cal, err} \quad (3.10)$$

mostly reaches values of  $\pm 1\%$ . The error of the calculated traversing angles

$$\alpha_{err} = \alpha_{cal} - \alpha_{trav} \quad (3.11a)$$

$$\beta_{err} = \beta_{cal} - \beta_{trav} \quad (3.11b)$$

is about  $\pm 1^\circ$  in most positions. For traversed angles from  $15^\circ$  and beyond  $20^\circ$  especially the pitch angle of the probe is insufficiently calculated, a fact that increases with Mach number and that has to be taken into account. Other deviations might depend on the slight pressure and temperature fluctuations in the tank.



#### 4. Conclusions

At the High-Speed Cascade Wind Tunnel of the University of the Federal Armed Forces Munich a fully computer controlled measurement system for three dimensional hot-film anemometry has been established. With the new data acquisition system all measured data are directly digitized and stored on a hard disk.

For the operation of the data acquisition system a software package (SMASH) was designed for modularity and flexibility to the various test conditions. The program provides all control and acquisition functions for the calibration of a triple hot-film probe as well as for measurements behind or in between the cascade.

An extensive test program showed the accuracy and the reproducibility of the data acquisition system. The dominant influences on the calibration results are tank pressure and ambient temperature of the probe. Temperature fluctuations and deviations between calibration and measurement are compensated and a correction method for pressure deviation will be introduced.

The sensor position in the probe-fixed coordinate system and the free stream Mach number dominates the behavior of the directional characteristic and thus the quality of the mathematical approximation using an approach that is independent of the knowledge of the actual probe geometry.

Detailed investigations concerning different probe geometries and improvements of the directional calibration at high Mach numbers are necessary. Assuming a shortcoming of the approximation to model the measured characteristics the procedure including the evaluation of flow properties will be tested furthermore.

#### 5. Acknowledgements

The authors gratefully acknowledge the Institut für Experimentelle Strömungsmechanik of the DLR Göttingen especially Dr. H.-P. Kreplin and Dr. H. Rosemann who developed the calibration procedure and the evaluation program modules for their support.

#### 6. References

- /1/ Sturm, W., Fottner, L.  
The High-Speed Cascade Wind Tunnel of the German Armed Forces University Munich;  
Paper presented at the 8th Symposium on Measuring Techniques for Transonic and Supersonic Flows in Cascades and Turbomachines, Genoa (1985)
- /2/ Römer, K., Ladwig, M., Fottner, L.  
Measuring Techniques at the High-Speed Cascade Wind Tunnel of the University of the Federal Armed Forces Munich;  
Paper presented at the 9th Symposium on Measuring Techniques for Transonic and Supersonic Flows in Cascades and Turbomachines, Oxford (1988)
- /3/ Wunderwald, D.  
Untersuchungen der Turbulenzstrukturen in hochbelasteten Verdichter- und Turbinengittern;  
Institutsbericht LRT-WE 12-92/06, Institut für Strahltriebwerke, UniBw München (1992)
- /4/ Wilfert, G.  
Mischungsvorgänge zwischen Kühlfilmern und Grenzschichten fortschrittlicher Turbinenbeschleunigungen;  
Institutsbericht LRT-WE 12-92/08, Institut für Strahltriebwerke, UniBw München (1992)
- /5/ Wilfert, G., Ladwig, M., Fottner, L.  
PANDA - A new Data Acquisition System for Wake and Profile Pressure Distribution Measurements at the High-Speed Cascade Wind Tunnel;  
Paper presented at the 10th Symposium on Measuring Techniques for Transonic and Supersonic Flows in Cascades and Turbomachines, Brüssel (1990)
- /6/ Hoffacker, H.  
Konzeption und Erprobung der Steuerung des Traversiergeräts im Hochgeschwindigkeits-Gitterwindkanal;  
Diplomarbeit Nr. 86/18, Institut für Strahltriebwerke, UniBw München (1986)
- /7/ Pape, O.  
Konzeption und Erprobung einer automatischen Sondensteuerung für mehrdimensionale Heißfühler-Messungen;  
Studienarbeit Nr. 91/3.3; Institut für Strahltriebwerke, UniBw München (1991)

- /8/ Rosemann, H.  
Einfluß der Geometrie von Mehrfach-Hitzdrahtsonden auf die Meßergebnisse in turbulenten Strömungen;  
Institut für Experimentelle Strömungsmechanik, DLR Göttingen, (1989)
- /9/ King, L. V.  
On the Convection of Heat from Small Cylinders in a Stream of Fluid: Determination of the Convection Constants of Small Platinum Wires, with Application to Hot Wire Anemometry;  
Philosophical Transactions of the Royal Society, A/214, London (1914)
- /10/ Jørgensen, F. E.  
Directional Sensitivity of Wire and Fiber Film Probes;  
DISA Information No. 11 (1971)
- /11/ Wunderwald, D.  
Untersuchung verschiedener Einflußparameter auf die Geschwindigkeits- und Richtungskalibrierung von Tripel-Heißfilmsonden;  
Institutsbericht LRT-WE 12-92/13, Institut für Strahlantriebe, UniBw München (1992)
- /12/ Lomas, C. G.  
Fundamentals of Hot Wire Anemometry;  
Cambridge University Press, Cambridge (1986)
- /13/ Strickert, H.  
Hitzdraht- und Hitzfilmanemometrie;  
VEB Verlag Technik, Berlin (1974)
- /14/ Bearman, P. W.  
Corrections for the Effect of Ambient Temperature Drift on Hot-Wire Measurements in Incompressible Flow;  
DISA-Information No. 11 (1971)
- /15/ Kanevce, G., Oka, S.  
Correcting Hot-Wire Readings for Influence of Fluid Temperature Variations;  
DISA-Information No. 15 (1973)

## 7. List of Figures

- Fig. 1.1: The High-Speed Cascade Wind Tunnel  
Fig. 2.1: Schematic view of the constant temperature anemometry  
Fig. 2.2: Triple probes, the coordinate system and the test object  
Fig. 2.3: Setup of the 3D-Hot-Film Anemometry  
Fig. 2.4: Data flow of the anemometer signals  
Fig. 2.5: Peripheral Data Acquisition System  
Fig. 2.6: Schematic view of the traversing system  
Fig. 2.7: Traversing arm with standard triple probe, prandtl- and temperature probe  
Fig. 2.8: SMASH modules and screen menus  
Fig. 3.1: Velocity calibrations at different tank pressures and temperatures  
Fig. 3.2: Velocity calibration using a temperature compensation  
Fig. 3.3: Comparison of a triple wire probe and a triple film probe  
Fig. 3.4: Directional characteristics of the tested probes  
Fig. 3.5: Directional characteristics for different parameters  
Fig. 3.6: Directional characteristics for different Mach numbers  
Fig. 3.7: Adjusted surfaces and relative error of the effective cooling velocity  
Fig. 3.8: Evaluation of calibration data for flow properties

<b>UniBw München</b> Institut für Strahltriebwerke	<b>High-Speed Cascade Wind Tunnel</b>	<b>1985</b>																																																		
<table border="0"> <tr> <td colspan="3"><u>test section data:</u></td> <td colspan="3"><u>supply units:</u></td> <td colspan="3"><u>wind tunnel data:</u></td> </tr> <tr> <td>- Mach number</td> <td>: <math>0.2 \leq Ma \leq 1.05</math></td> <td>- evacuating unit</td> <td>: <math>P_1 = 30 \text{ kW}</math></td> <td>- AC electric motor</td> <td>: <math>P = 1300 \text{ kW}</math></td> </tr> <tr> <td>- Reynolds number</td> <td>: <math>0.2 \cdot 10^6 \text{ m}^{-1} \leq Re/l \leq 16.0 \cdot 10^6 \text{ m}^{-1}</math></td> <td><math>P_2 = 20 \text{ kW}</math></td> <td>- boundary layer suction</td> <td>: <math>P = 155 \text{ kW}</math></td> <td>- axial compressor</td> <td>: 6 stages</td> </tr> <tr> <td>- degree of turbulence</td> <td>: <math>0.4\% \leq Tu_1 \leq 7.5\%</math></td> <td>(centrifugal compressor)</td> <td>- additional air supply</td> <td>: <math>P = 1000 \text{ kW}</math></td> <td>air flow rate</td> <td>: <math>V_{\text{max}} = 30 \text{ m}^3/\text{s}</math></td> </tr> <tr> <td>- upstream flow angle</td> <td>: <math>25^\circ \leq \beta_1 \leq 155^\circ</math></td> <td>(screw compressor)</td> <td></td> <td></td> <td>total pressure ratio</td> <td>: <math>(p_{t1}/p_k)_{\text{max}} = 2.14</math></td> </tr> <tr> <td>- blade height</td> <td>: 300 mm</td> <td></td> <td></td> <td></td> <td>number of revolutions</td> <td>: <math>n_{\text{max}} = 6300 \text{ min}^{-1}</math></td> </tr> <tr> <td>- test section height</td> <td>: 235 mm - 510 mm</td> <td></td> <td></td> <td></td> <td>tank pressure</td> <td>: <math>p_k = 0.04 - 1.2 \text{ bar}</math></td> </tr> </table>			<u>test section data:</u>			<u>supply units:</u>			<u>wind tunnel data:</u>			- Mach number	: $0.2 \leq Ma \leq 1.05$	- evacuating unit	: $P_1 = 30 \text{ kW}$	- AC electric motor	: $P = 1300 \text{ kW}$	- Reynolds number	: $0.2 \cdot 10^6 \text{ m}^{-1} \leq Re/l \leq 16.0 \cdot 10^6 \text{ m}^{-1}$	$P_2 = 20 \text{ kW}$	- boundary layer suction	: $P = 155 \text{ kW}$	- axial compressor	: 6 stages	- degree of turbulence	: $0.4\% \leq Tu_1 \leq 7.5\%$	(centrifugal compressor)	- additional air supply	: $P = 1000 \text{ kW}$	air flow rate	: $V_{\text{max}} = 30 \text{ m}^3/\text{s}$	- upstream flow angle	: $25^\circ \leq \beta_1 \leq 155^\circ$	(screw compressor)			total pressure ratio	: $(p_{t1}/p_k)_{\text{max}} = 2.14$	- blade height	: 300 mm				number of revolutions	: $n_{\text{max}} = 6300 \text{ min}^{-1}$	- test section height	: 235 mm - 510 mm				tank pressure	: $p_k = 0.04 - 1.2 \text{ bar}$
<u>test section data:</u>			<u>supply units:</u>			<u>wind tunnel data:</u>																																														
- Mach number	: $0.2 \leq Ma \leq 1.05$	- evacuating unit	: $P_1 = 30 \text{ kW}$	- AC electric motor	: $P = 1300 \text{ kW}$																																															
- Reynolds number	: $0.2 \cdot 10^6 \text{ m}^{-1} \leq Re/l \leq 16.0 \cdot 10^6 \text{ m}^{-1}$	$P_2 = 20 \text{ kW}$	- boundary layer suction	: $P = 155 \text{ kW}$	- axial compressor	: 6 stages																																														
- degree of turbulence	: $0.4\% \leq Tu_1 \leq 7.5\%$	(centrifugal compressor)	- additional air supply	: $P = 1000 \text{ kW}$	air flow rate	: $V_{\text{max}} = 30 \text{ m}^3/\text{s}$																																														
- upstream flow angle	: $25^\circ \leq \beta_1 \leq 155^\circ$	(screw compressor)			total pressure ratio	: $(p_{t1}/p_k)_{\text{max}} = 2.14$																																														
- blade height	: 300 mm				number of revolutions	: $n_{\text{max}} = 6300 \text{ min}^{-1}$																																														
- test section height	: 235 mm - 510 mm				tank pressure	: $p_k = 0.04 - 1.2 \text{ bar}$																																														

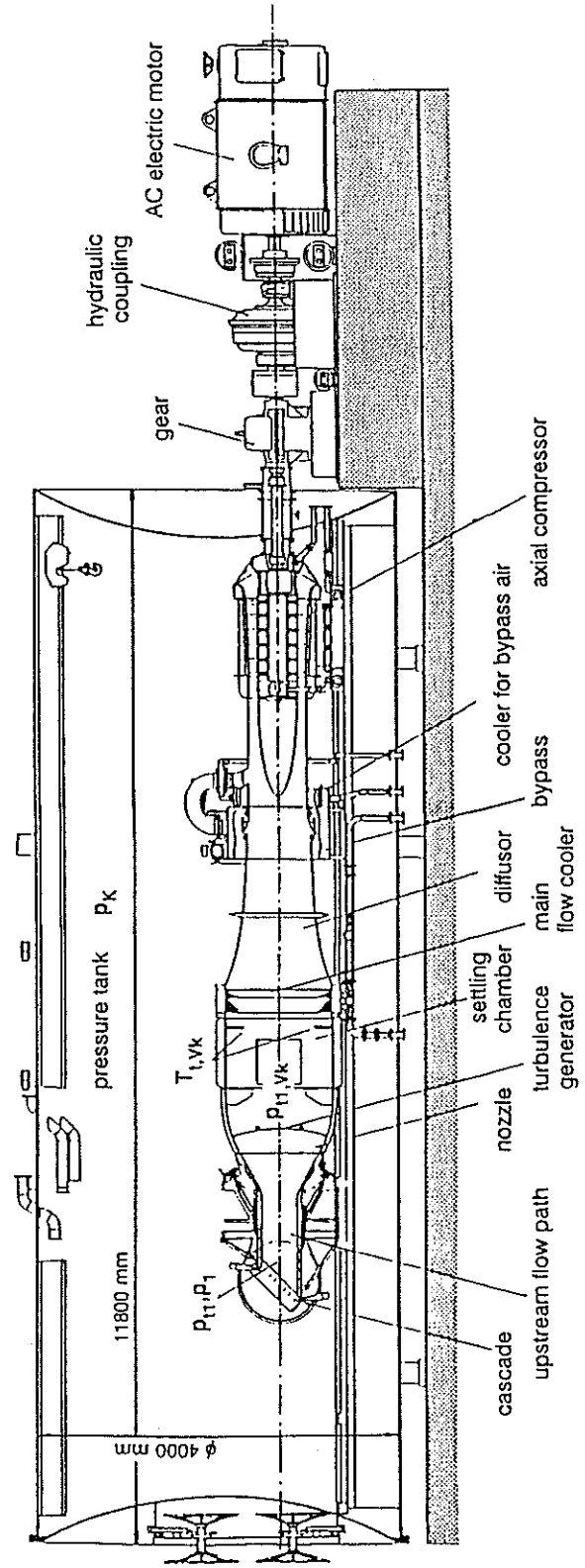


Fig. 1.1: The High-Speed Cascade Wind Tunnel

---

## Constant - Temperature - Anemometer

---

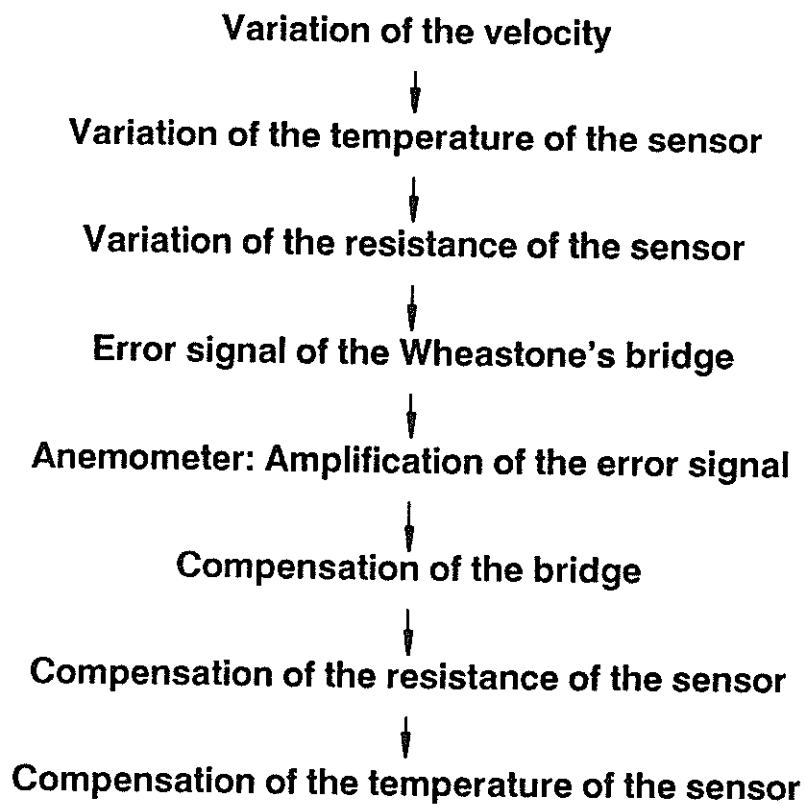
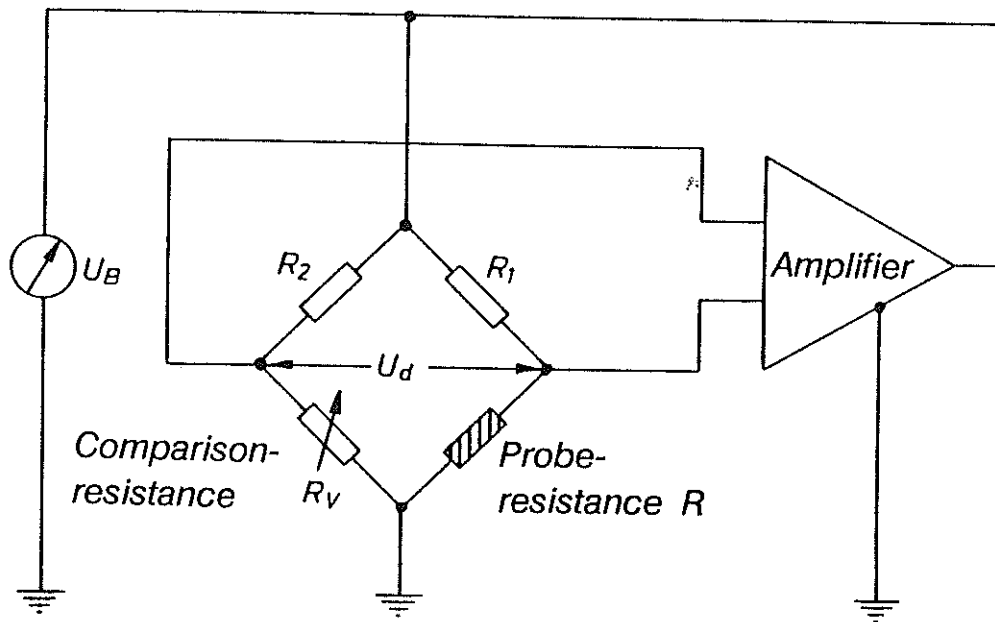
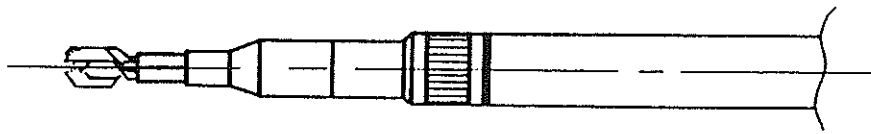


Fig. 2.1: Schematic view of the constant temperature anemometry



Dantec 55 R 91



Subminiature triple probe

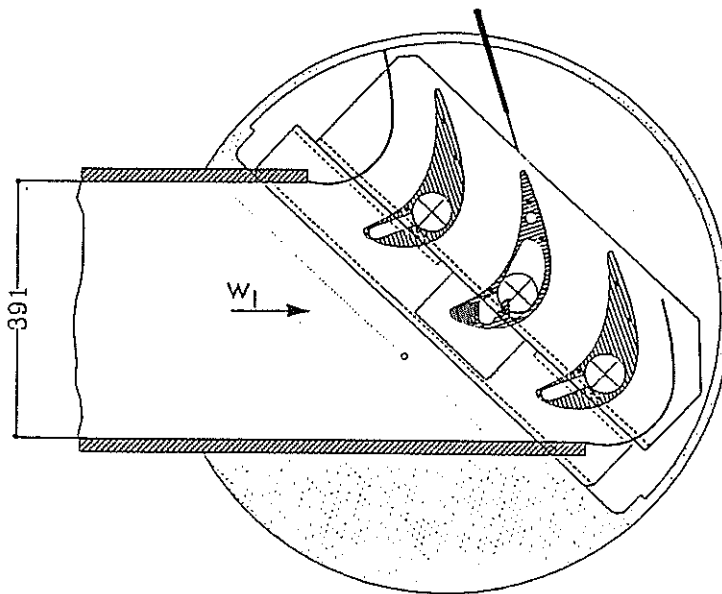
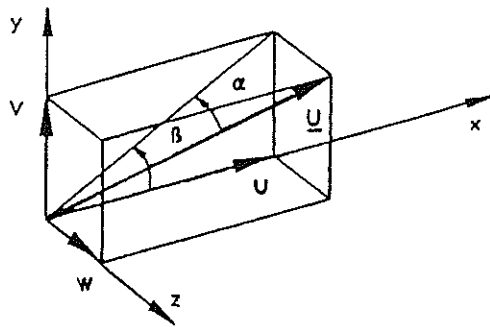


Fig. 2.2: Triple probes, coordinate system and test object

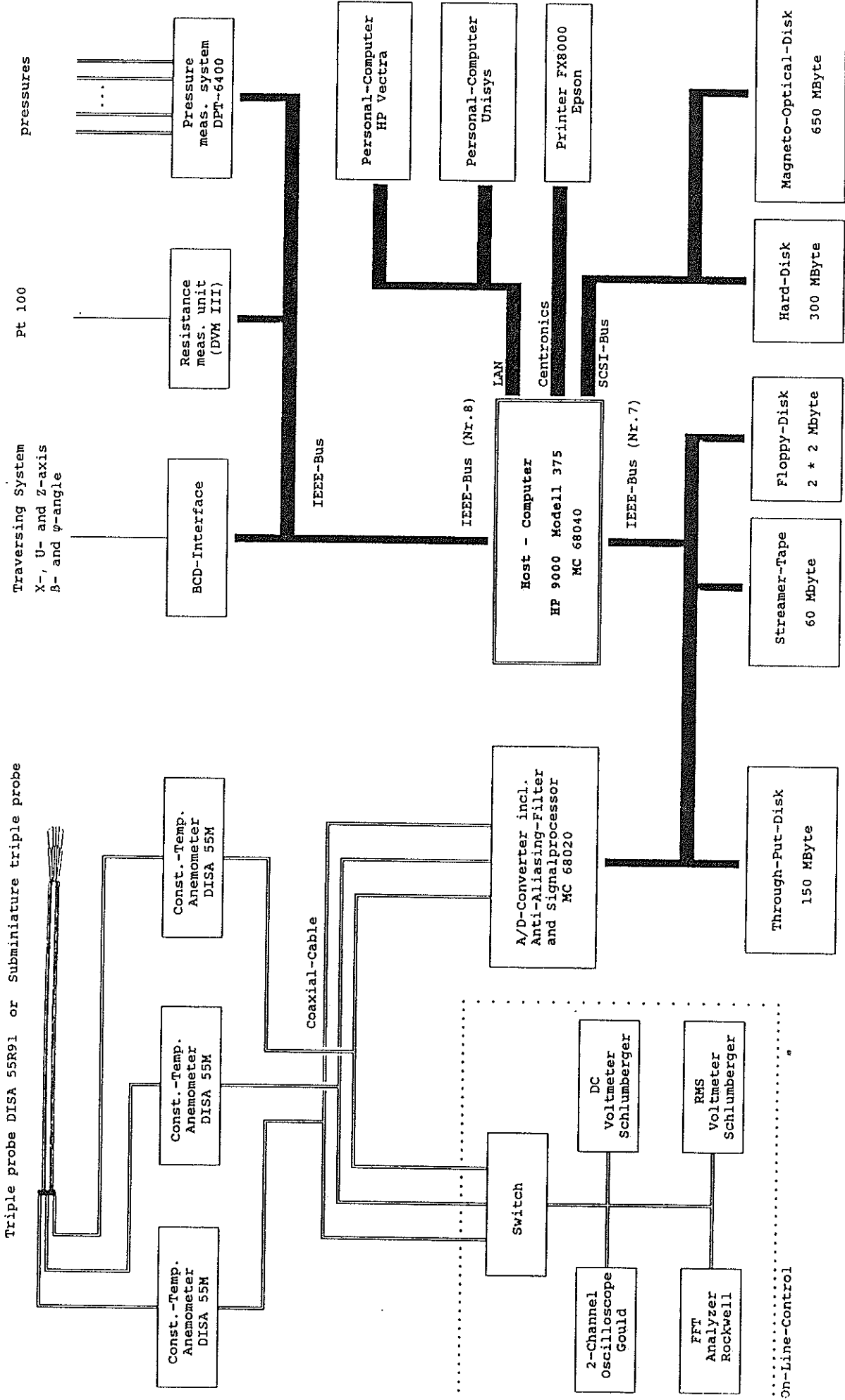


Fig. 2.3: Setup of the 3D-Hot-Film-Anemometry

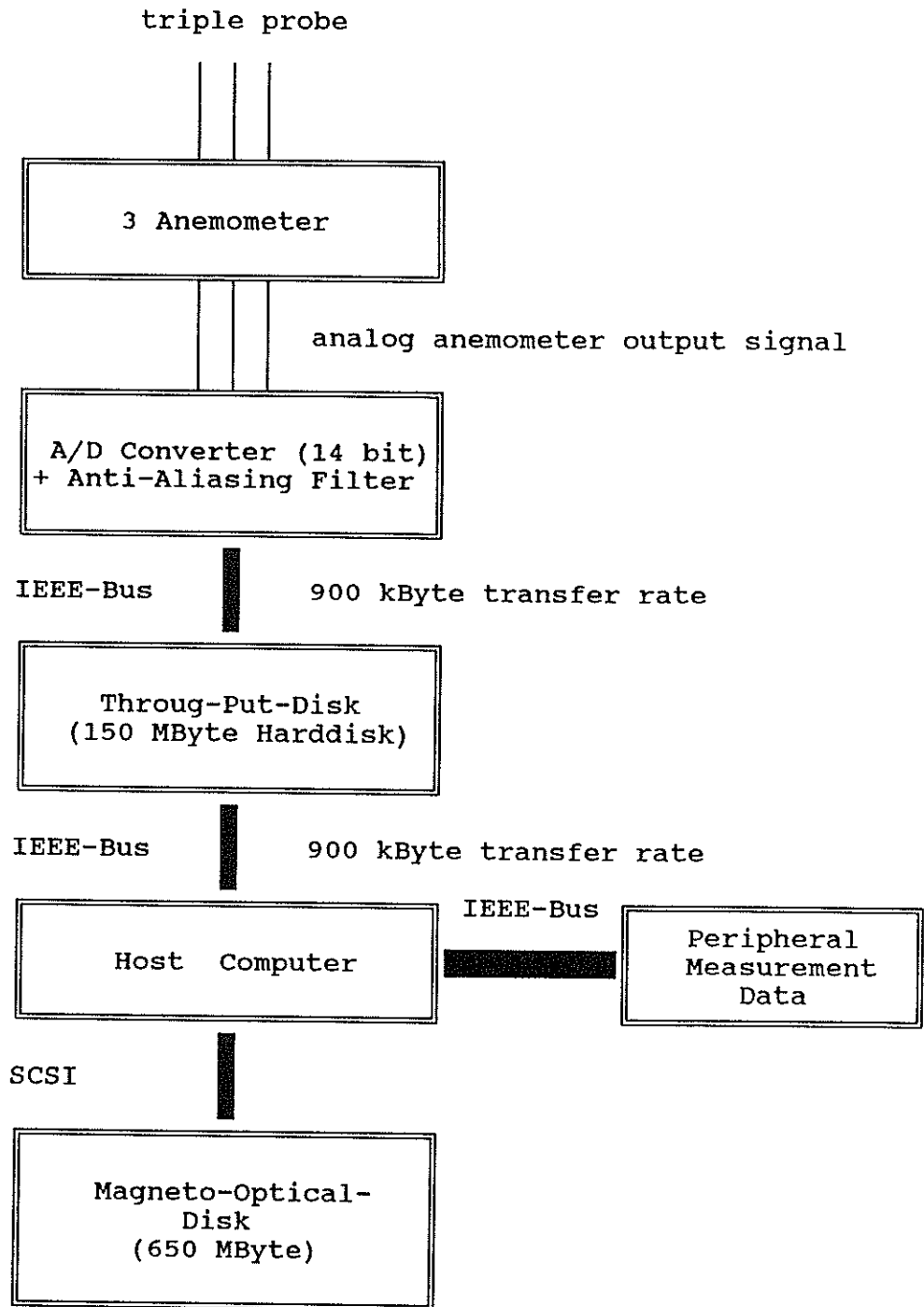


Fig. 2.4: Data flow of the anemometer signals

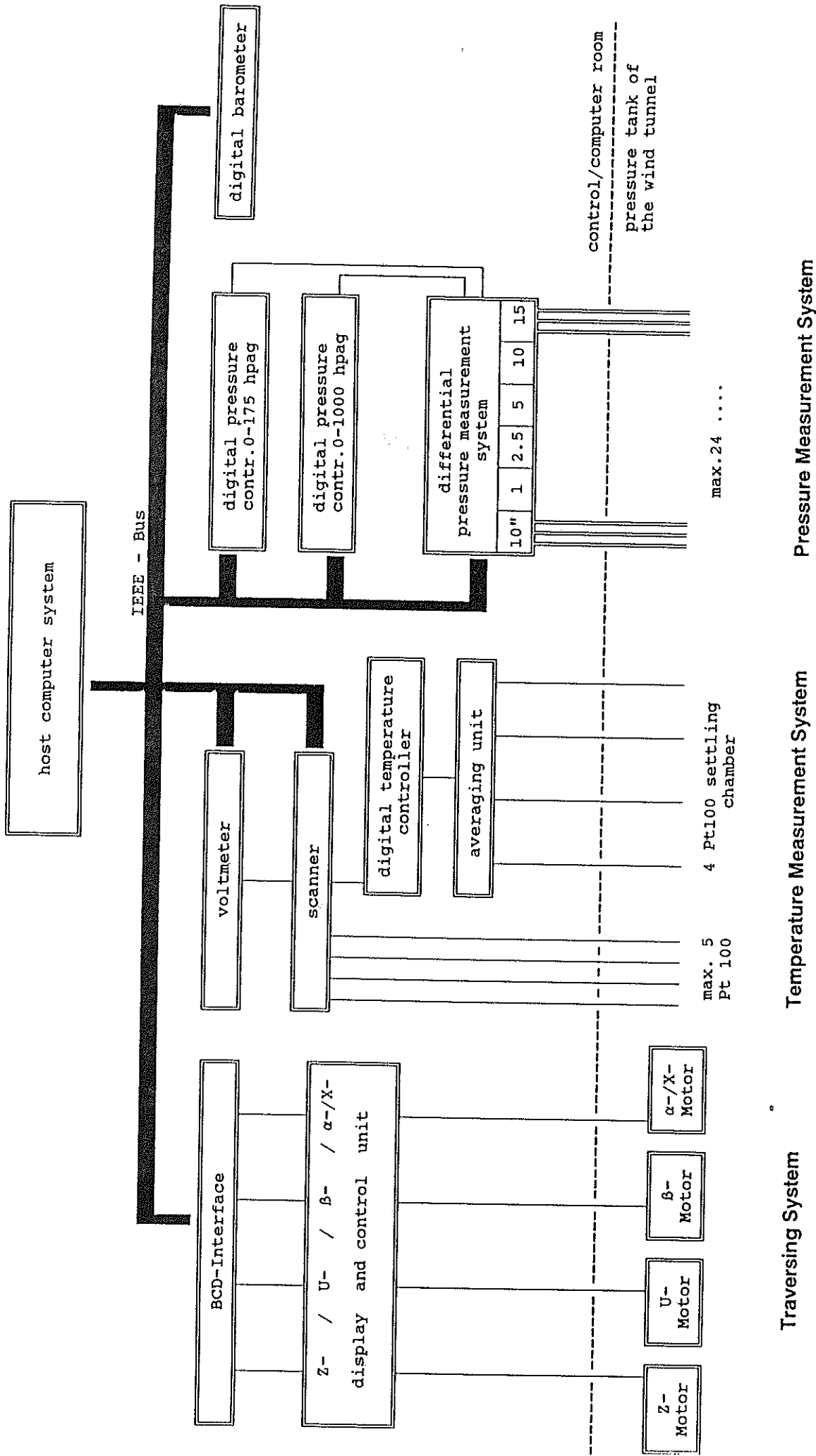


Fig. 2.5: Peripheral Data Acquisition System



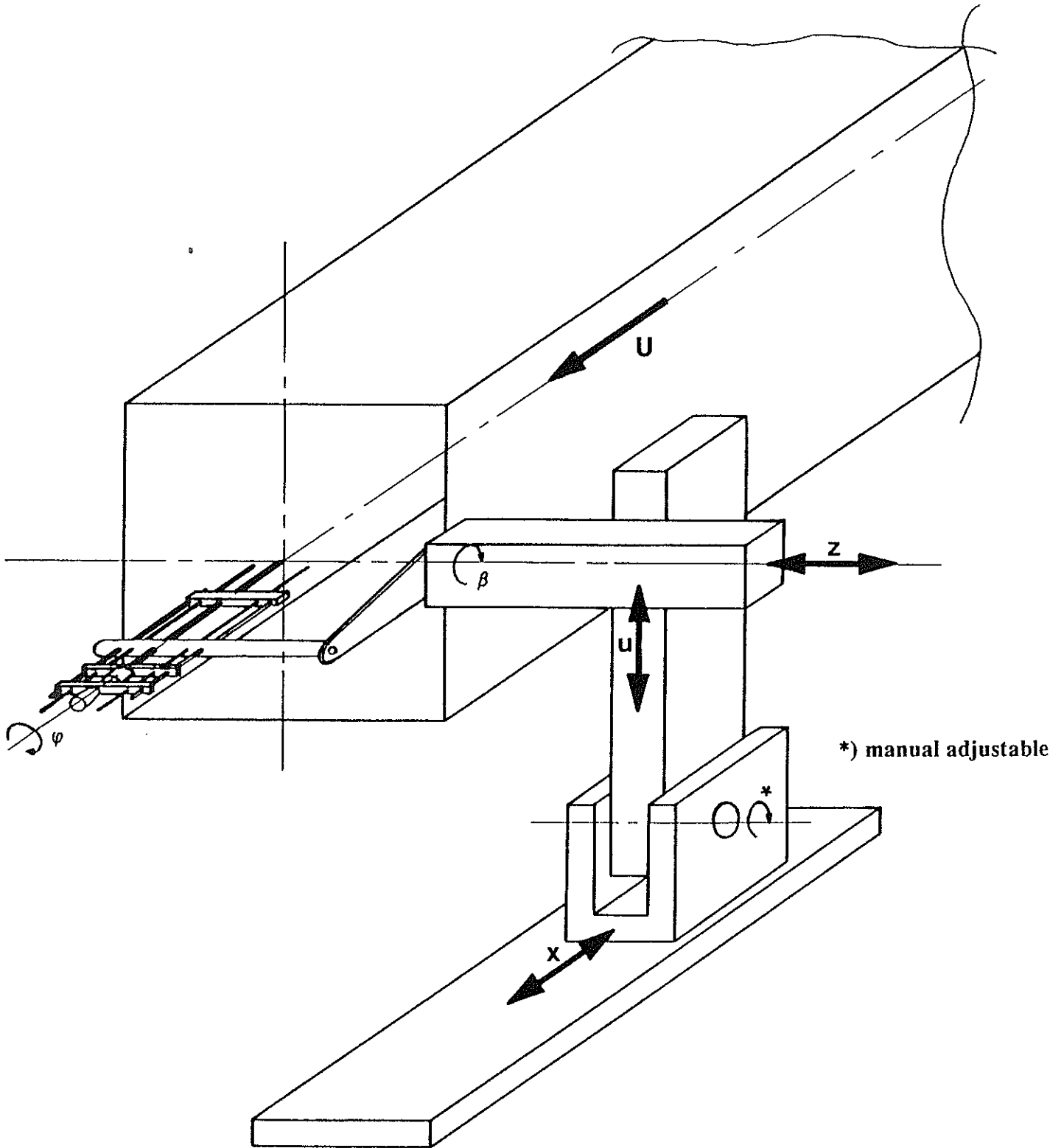


Fig. 2.6: Schematic view of the traversing system

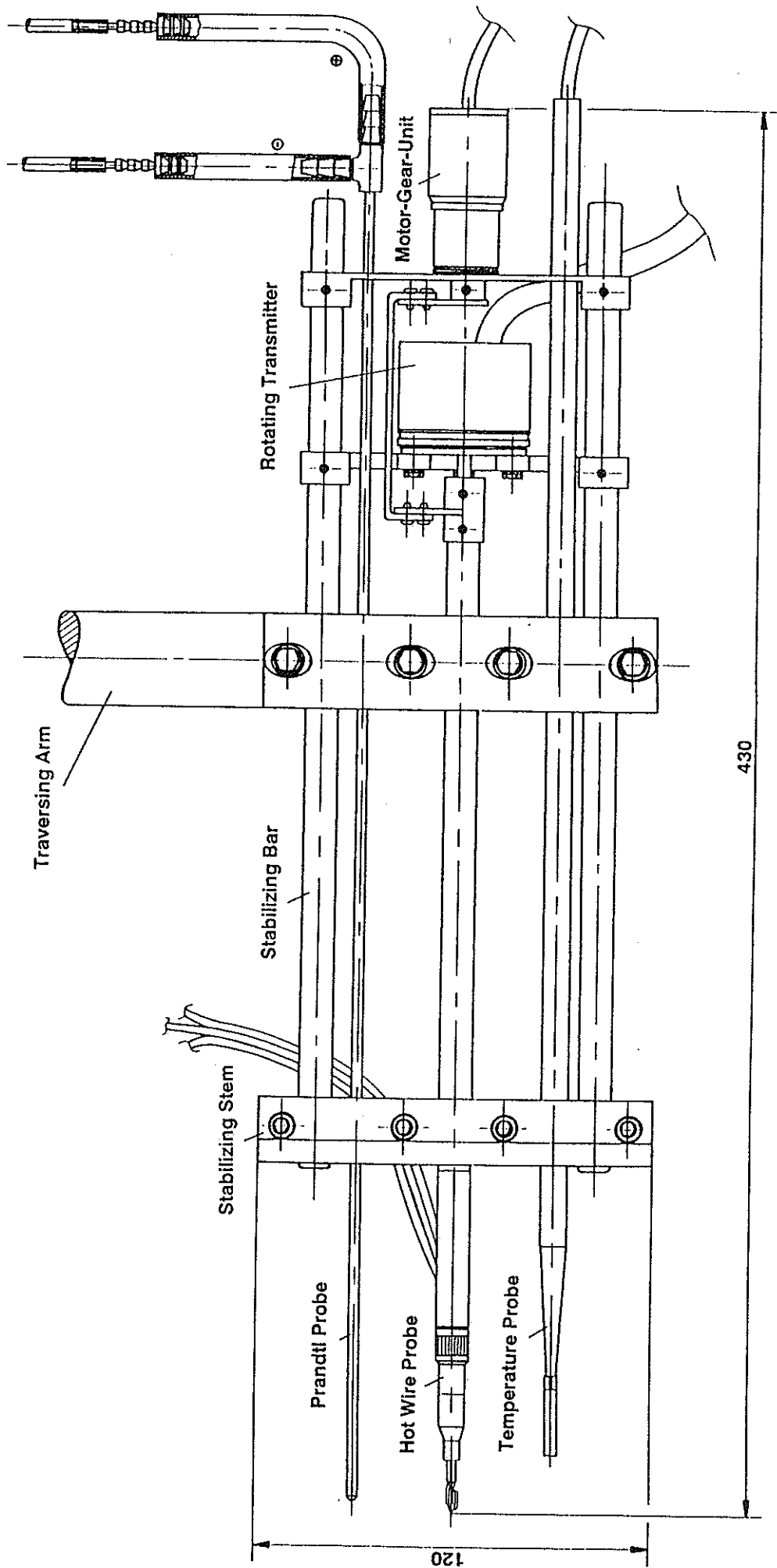


Fig. 2.7: Traversing arm with standard triple probe, prandtl- and temperature probe

```

****      SMASH      ****
Software for Measurement and Analytical Evaluation
of Signals from Hot-Sensor Anemometry

```

```

** Configuration Menu **

```

- \* Read configuration and cascade file
- \* Edit testspecific data
- \* Edit experimental set-up data and DPT-chart
- \* Check cascade data
- > Go back to main menu

```

** Calibration Menu **

```

- \* Read existing calibration file
- \* Make new calibration file
- \* Velocity calibration
- \* Directional calibration
- \* Off-line evaluation
- \* DPT-zero-calibration
- \* DPT-full-calibration
- > Go back to main menu

```

** Measurement Menu **

```

- \* Run a measurement program
- \* Test measurement at the current position
- \* Listing of the Through-Put Disk
- \* Re-initiate the equipment
- > Go back to main menu

```

** Evaluation **

```

(Calculation of the velocity vector,  
its absolute value and direction)

(Calculation of second order correlations)

```

** Print Menu **

```

- \* Print current configuration data
- \* Print current cascade data
- \* Print current calibration coefficients
- \* Print current evaluation results
- \* Print a file \*.cfg
- \* Print a file \*.git
- \* Print a file \*.cal
- \* Print a file \*.erg
- \* Run an operating system command
- > Go back to main menu

Fig. 2.8: SMASH modules and screen menus

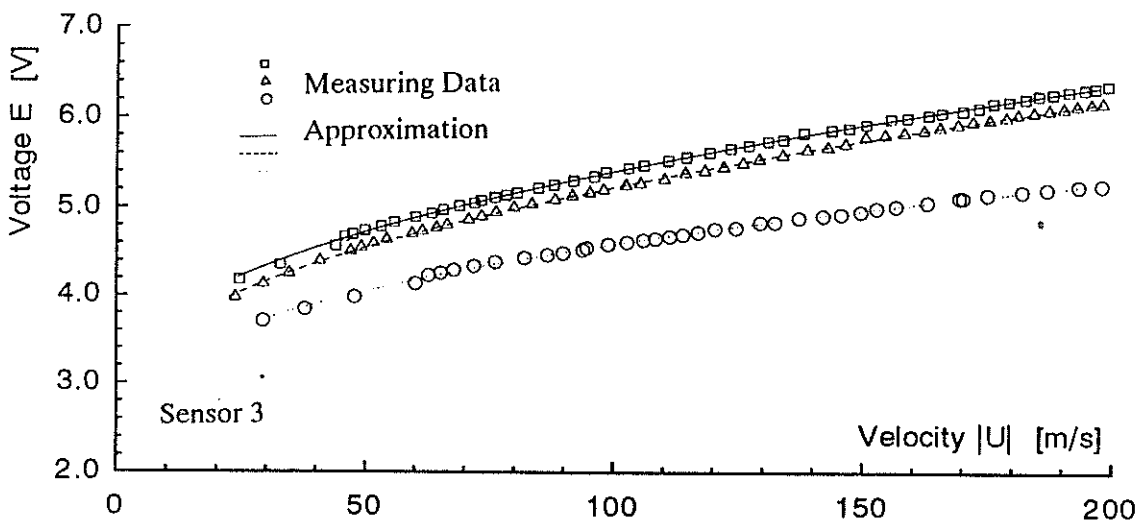
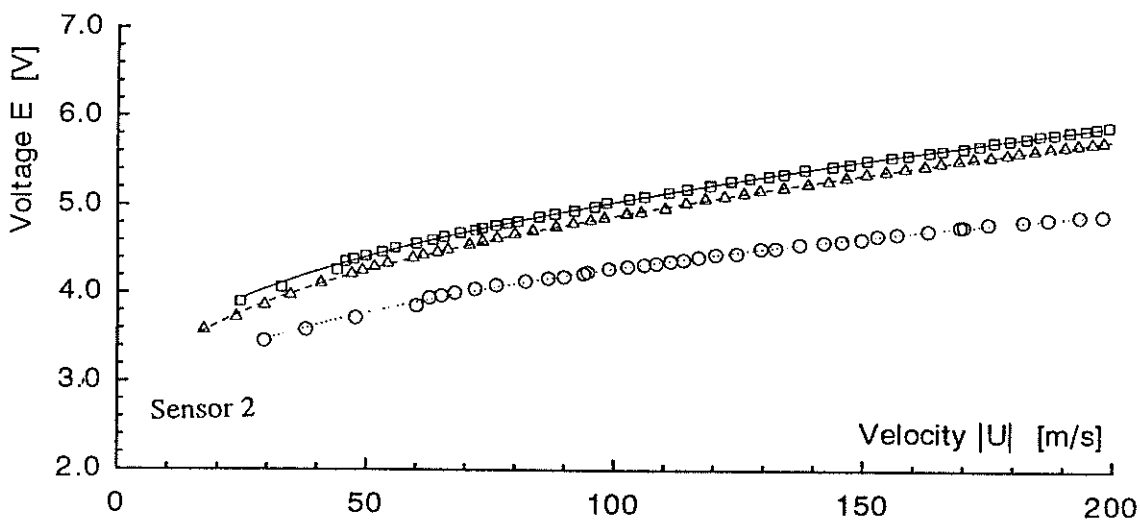
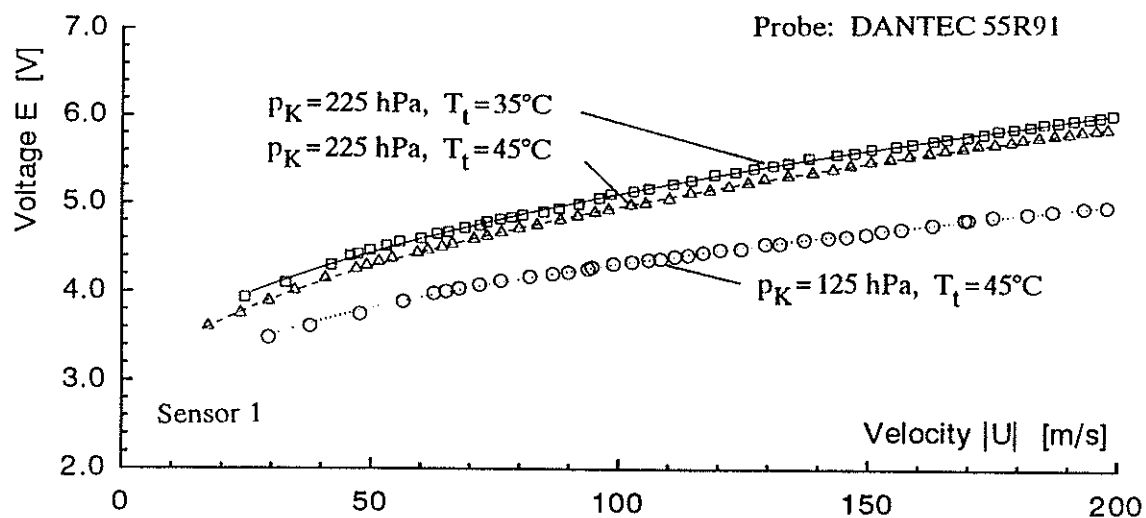


Fig. 3.1: Velocity calibrations at different tank pressures  $p_K$  and temperatures  $T_t$

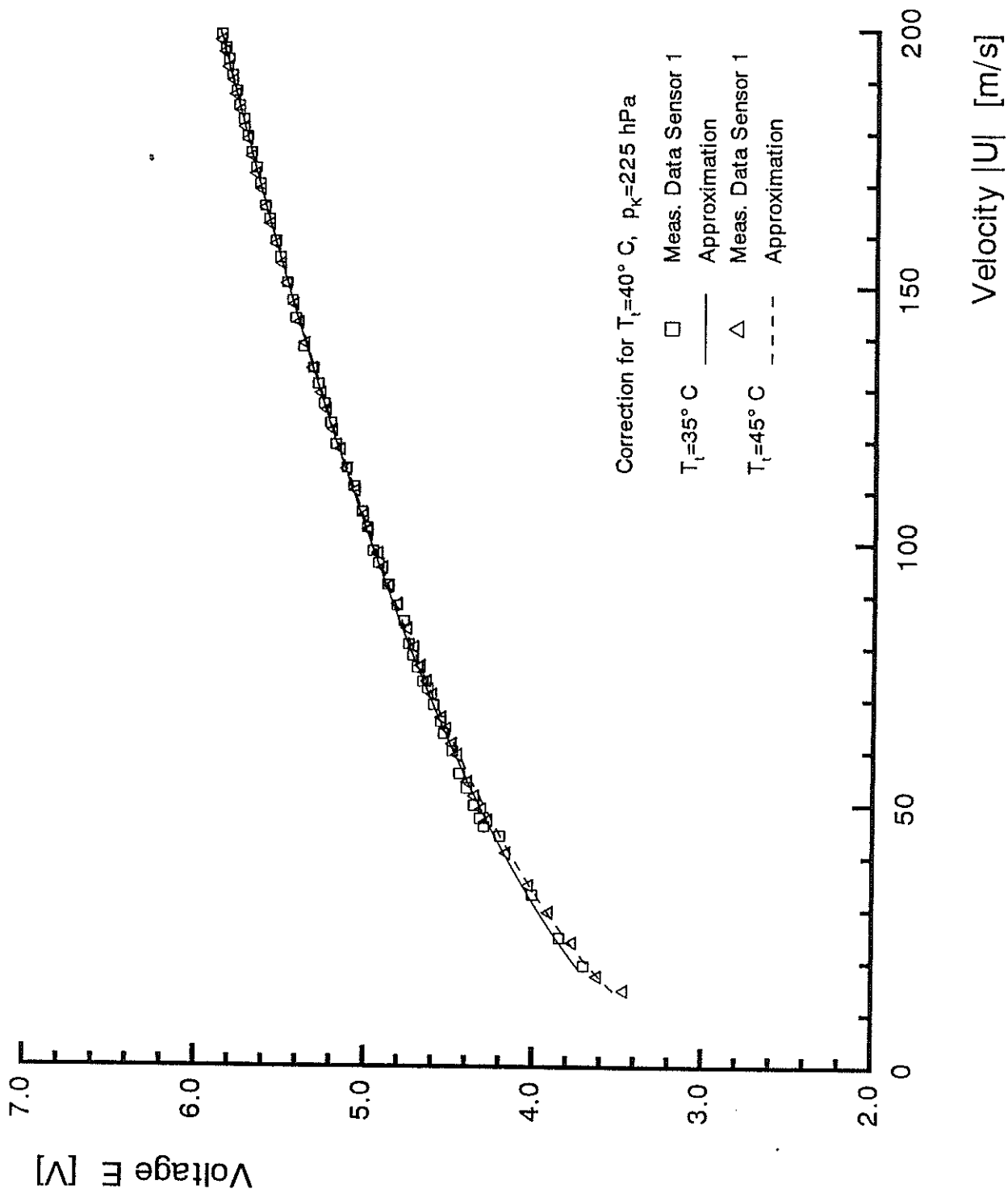


Fig. 3.2: Velocity calibration using a temperature compensation

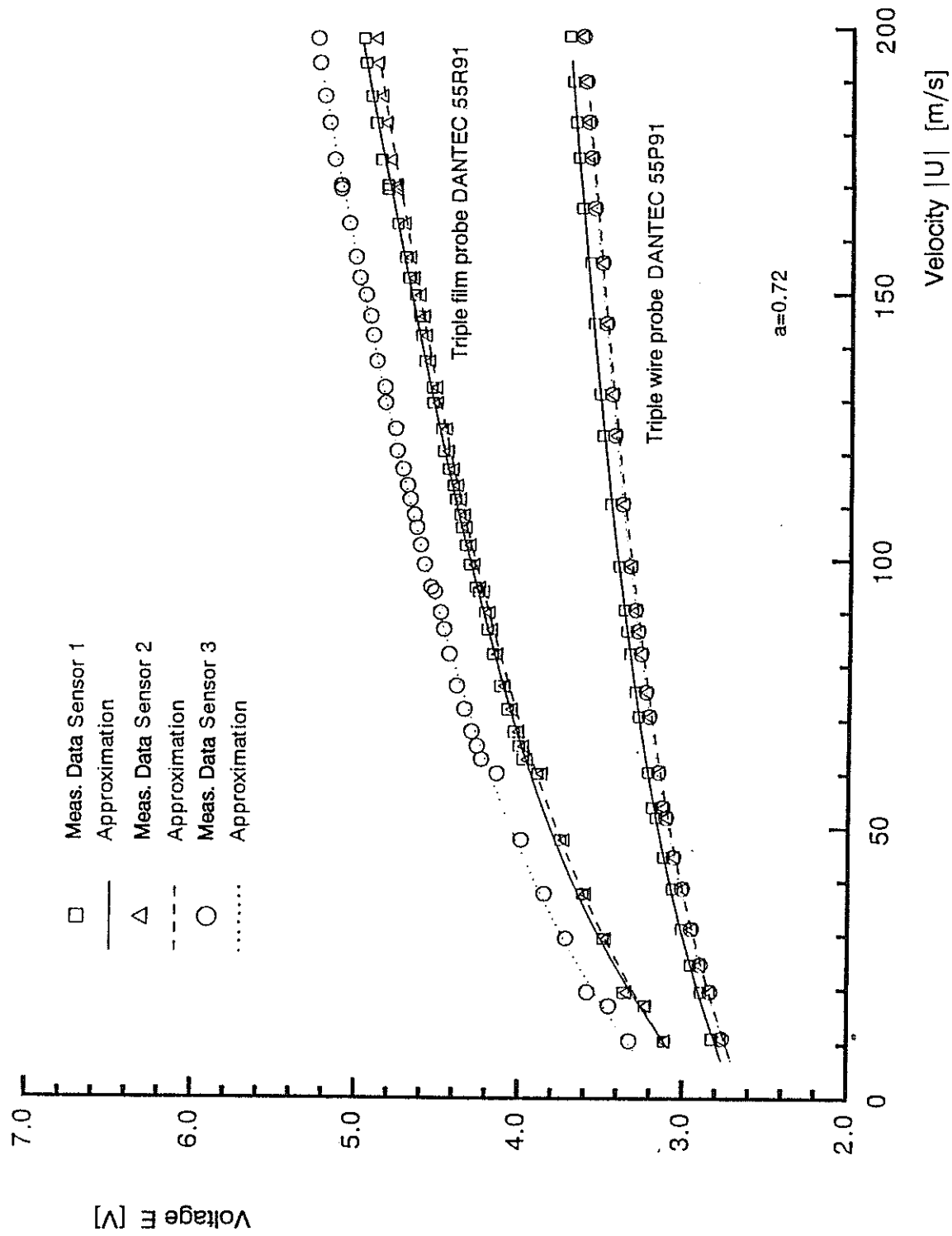
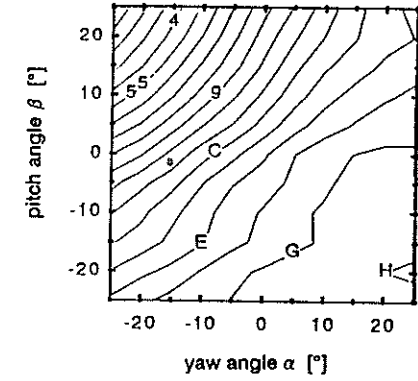


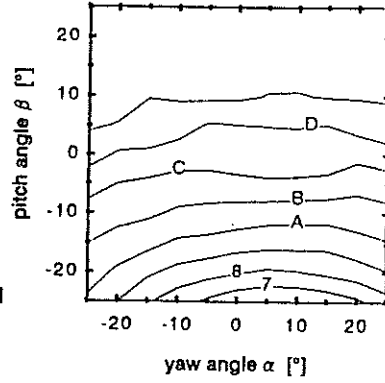
Fig. 3.3: Comparison of a triple wire probe and a triple film probe

probe: 55P91  
 $p_K = 75 \text{ hPa}$   
 $T_{TVK} = 40^\circ\text{C}$

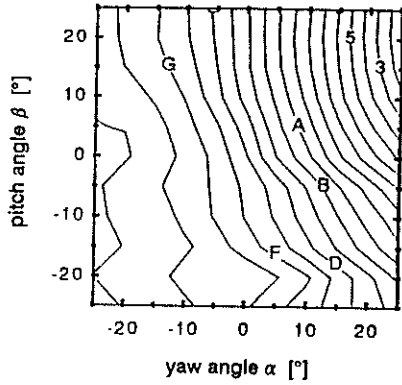
probe: 55R91  
 $p_K = 125 \text{ hPa}$   
 $T_{TVK} = 40^\circ\text{C}$



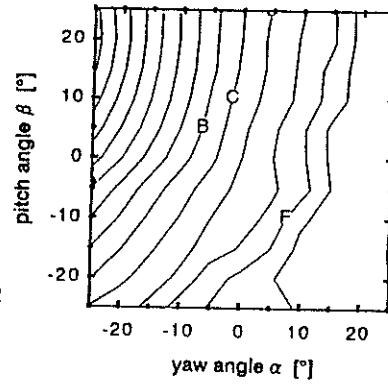
Sensor 1



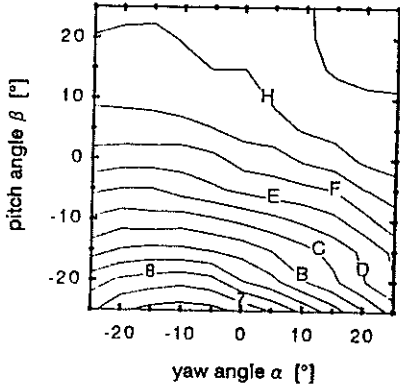
Level	UQG
J	1.30
I	1.25
H	1.20
G	1.15
F	1.10
E	1.05
D	1.00
C	0.95
B	0.90
A	0.85
9	0.80
8	0.75
7	0.70
6	0.65
5	0.60
4	0.55
3	0.50
2	0.45
1	0.40



Sensor 2



$t_S = 500 \text{ ms}$   
 $f_S = 65.5 \text{ kHz}$   
 $Ma = 0.6$



Sensor 3

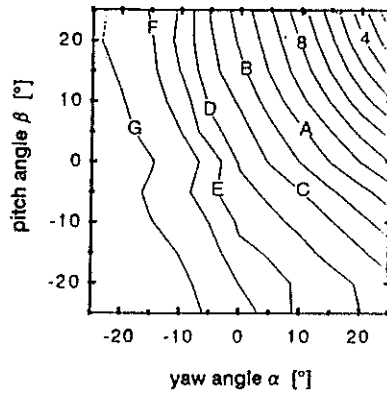


Fig. 3.4: Directional characteristics of the tested probes

probe: 55R91

$p_K = 225 \text{ hPa}$

$T_{TVK} = 40^\circ\text{C}$

$t_S = 500 \text{ ms}$

$f_S = 65.5 \text{ kHz}$

$Ma = 0.6$

$Tu = 3.5\%$

probe: 55R91

$p_K = 225 \text{ hPa}$

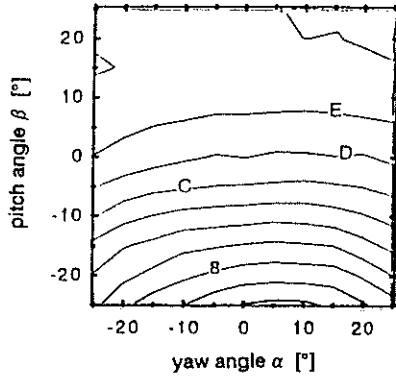
$T_{TVK} = 40^\circ\text{C}$

$t_S = 2000 \text{ ms}$

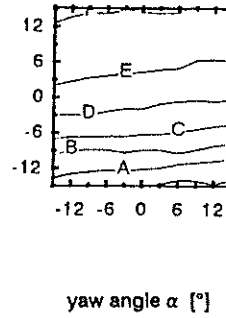
$f_S = 16.4 \text{ kHz}$

$Ma = 0.6$

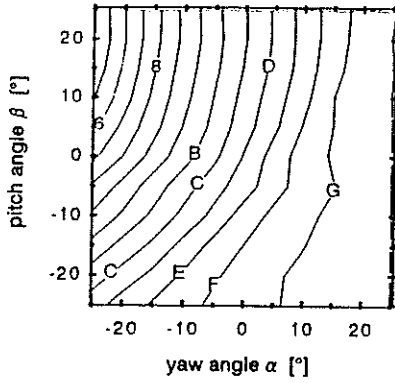
$Tu = 1.3\%$



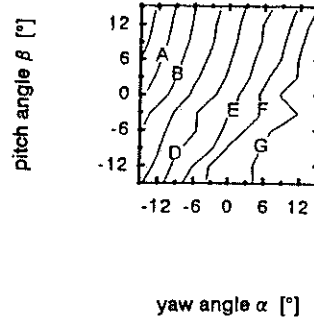
Sensor 1



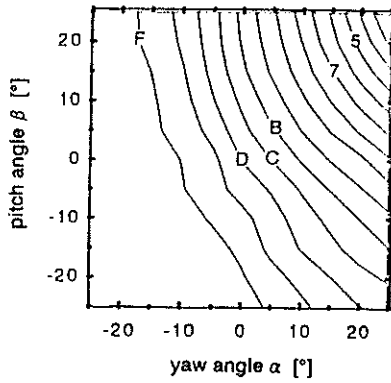
yaw angle  $\alpha$  [°]



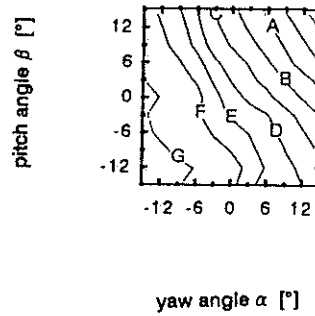
Sensor 2



yaw angle  $\alpha$  [°]



Sensor 3



yaw angle  $\alpha$  [°]

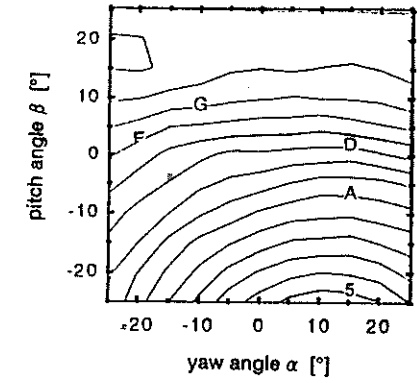
Level	UOG
J	1.30
I	1.25
H	1.20
G	1.15
F	1.10
E	1.05
D	1.00
C	0.95
B	0.90
A	0.85
9	0.80
8	0.75
7	0.70
6	0.65
5	0.60
4	0.55
3	0.50
2	0.45
1	0.40

Fig. 3.5: Directional characteristics for different parameters

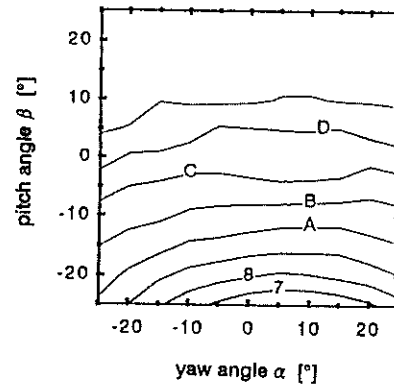


probe: 55R91  
 $p_K = 125 \text{ hPa}$   
 $T_{IVK} = 40^\circ\text{C}$   
 $Ma = 0.15$

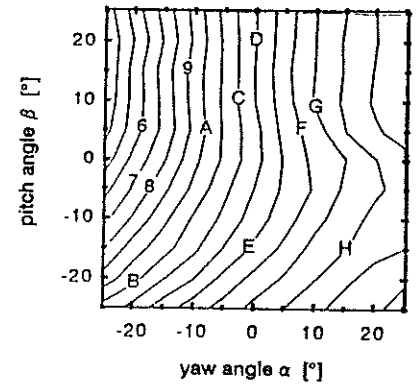
probe: 55R91  
 $p_K = 125 \text{ hPa}$   
 $T_{IVK} = 40^\circ\text{C}$   
 $Ma = 0.6$



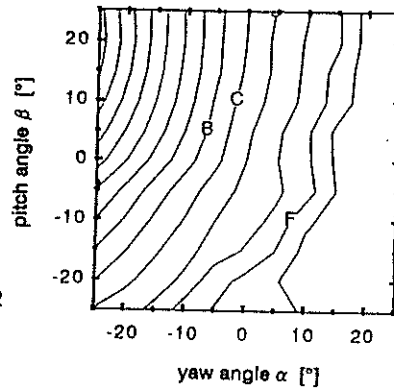
Sensor 1



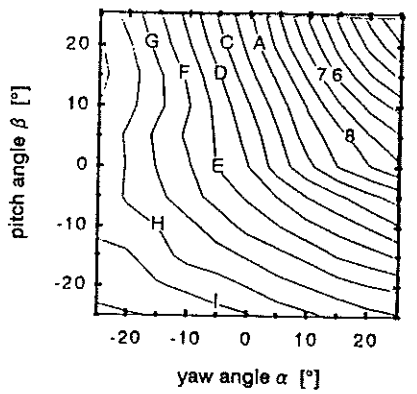
Level	UOG
J	1.30
I	1.25
H	1.20
G	1.15
F	1.10
E	1.05
D	1.00
C	0.95
B	0.90
A	0.85
9	0.80
8	0.75
7	0.70
6	0.65
5	0.60
4	0.55
3	0.50
2	0.45
1	0.40



Sensor 2



$t_S = 500 \text{ ms}$   
 $f_S = 65.5 \text{ kHz}$



Sensor 3

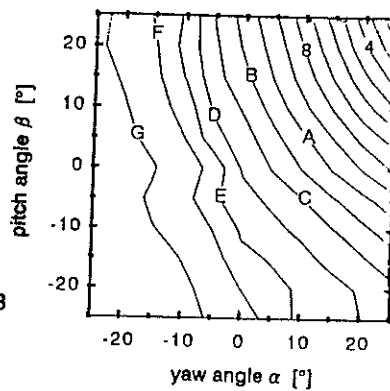
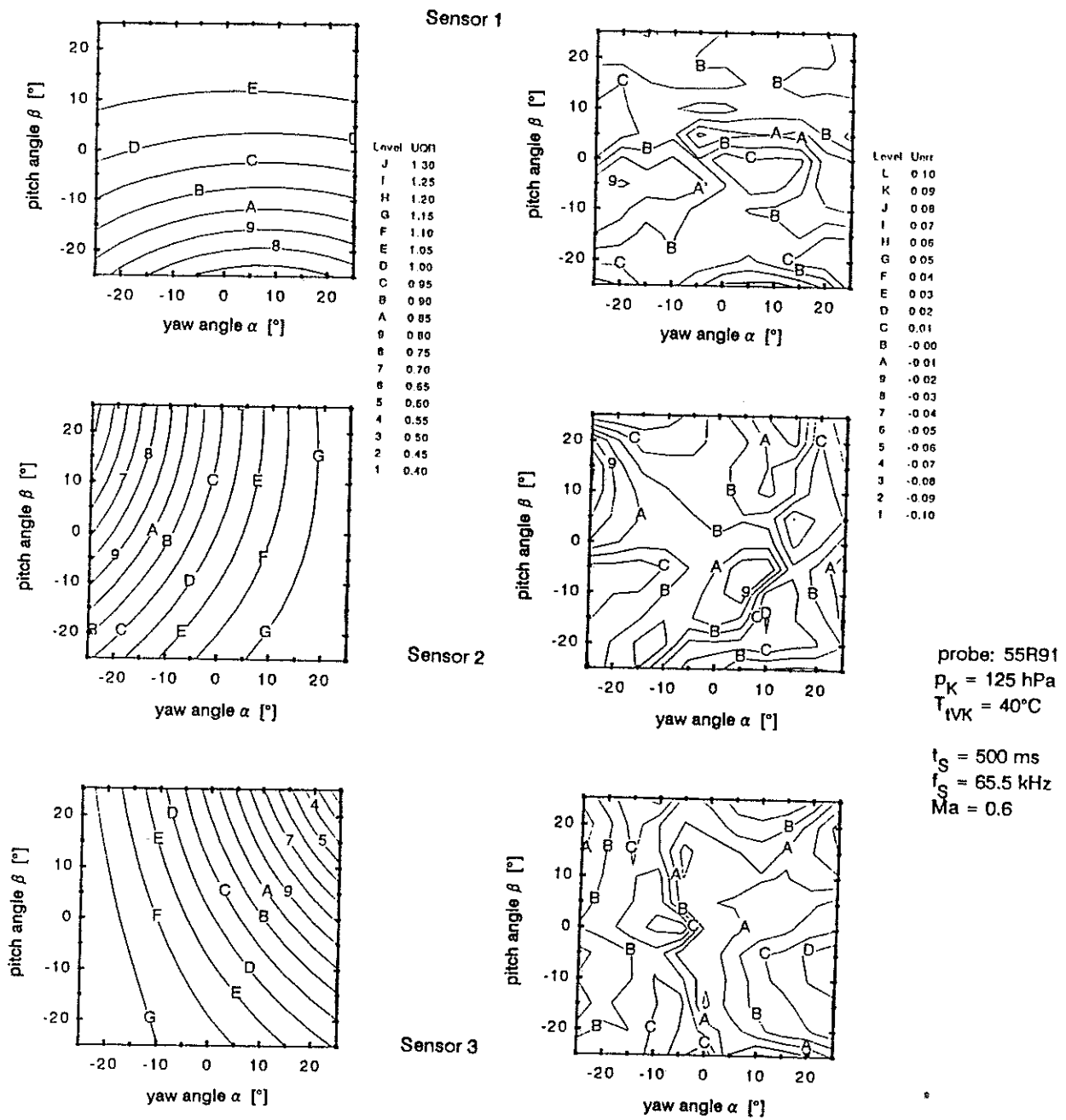


Fig. 3.6: Directional characteristics for different Mach numbers



**Fig. 3.7:** Adjusted surfaces and relative error of the effective cooling velocity

probe: 55R91

$p_K = 225 \text{ hPa}$

$T_{IVK} = 40^\circ\text{C}$

$t_S = 500 \text{ ms}$

$f_S = 65.5 \text{ kHz}$

$Ma = 0.6$

$Tu = 3.5\%$

probe: 55R91

$p_K = 225 \text{ hPa}$

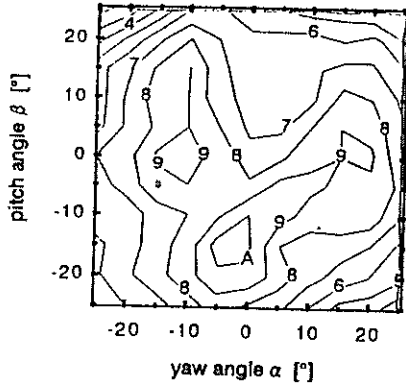
$T_{IVK} = 40^\circ\text{C}$

$t_S = 2000 \text{ ms}$

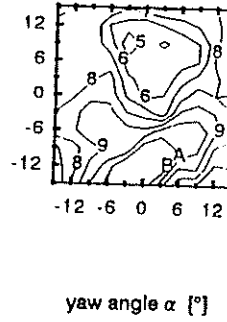
$f_S = 16.4 \text{ kHz}$

$Ma = 0.6$

$Tu = 1.3\%$



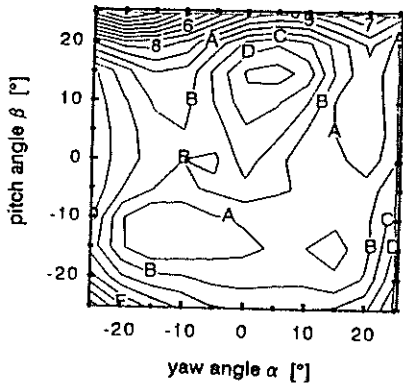
$U_{cal,err}$  in %



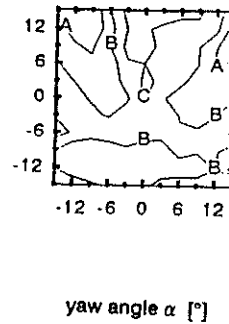
yaw angle  $\alpha$  [°]

Level  $U_{cal,err}$  in %

B	2.00
A	1.50
9	1.00
8	0.50
7	0.00
6	-0.50
5	-1.00
4	-1.50
3	-2.00
2	-2.50
1	-3.00



$\beta_{err}$  in °

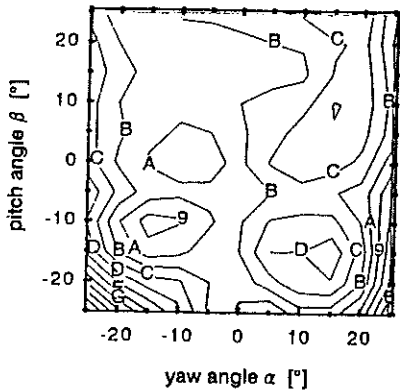


yaw angle  $\alpha$  [°]

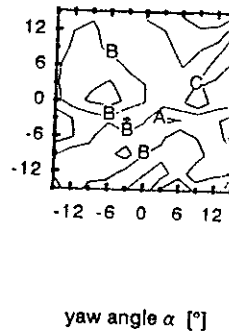
Level  $\beta_{err}$  in °

Level  $\alpha_{err}$  in °

L	10.00
K	9.00
J	8.00
I	7.00
H	6.00
G	5.00
F	4.00
E	3.00
D	2.00
C	1.00
B	0.00
A	-1.00
9	-2.00
8	-3.00
7	-4.00
6	-5.00
5	-6.00
4	-7.00
3	-8.00
2	-9.00
1	-10.00



$\alpha_{err}$  in °



yaw angle  $\alpha$  [°]

Fig. 3.8: Evaluation of calibration data for flow properties